IUCrData

ISSN 2414-3146

3-(2-Hydroxyethyl)-1-(4-nitrophenyl)-1*H*-benzo[*d*]-imidazol-3-ium bromide

Halliru Ibrahim,[a,b] Sizwe J. Zamisa,[b]* Muhammad D. Bala,[b] Pinkie Ntola[a] and Holger B. Friedrich[b]

[a]Department of Chemistry, Durban University of Technology, PO Box 1334, Durban, 4000, South Africa, and [b]School of Chemistry and Physics, University of KwaZulu-Natal, Private Bag X54001, Durban, 4000, South Africa. *Correspondence e-mail: zamisas@ukzn.ac.za

Received 29 November 2024
Accepted 2 December 2024

Edited by W. T. A. Harrison, University of Aberdeen, United Kingdom

Keywords: crystal structure; benzoimidazolium salt; tetramer.

CCDC reference: 2406833

Structural data: full structural data are available from iucrdata.iucr.org

The cation of the title salt, $C_{15}H_{14}N_3O_3^+\cdot Br^-$, has a dihedral angle of 24.26 (6)° between its fused imidazole and 4-nitrophenyl rings and the N—C—C—O torsion angle associated with the hydroxyethyl substituent is 60.15 (17)°. In the crystal, the bromide ions act as double acceptors for hydrogen bonds from a hydroxyl group (O—H···Br) and a fused imidazolium moiety (C—H···Br). Additionally, C—H···O hydrogen bonds between the phenyl group and hydroxyl oxygen atom create a two-dimensional supramolecular network extending diagonally in the crystallographic *bc* plane.

3D view

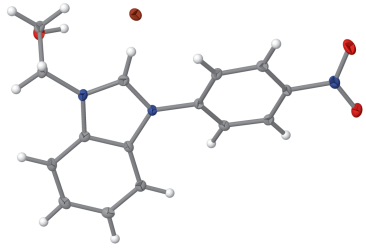

Chemical scheme

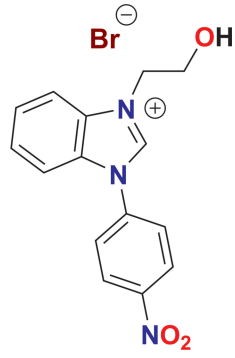

Structure description

The title compound is a benzimidazolylidene precursor based on the 1-(4-nitrophenyl) benzimidazol-3-yl scaffold (Lee *et al.*, 2004; Ibrahim *et al.*, 2022) and quaternized to form a 2-hydroxyethyl benzimidazolium bromide salt. Various works have reported the chemodosimetric potential of compounds with a fused 1*H*-benzo[*d*] backbone (Kumar *et al.*, 2013, 2015). The bulkiness of the backbone and the steric size of the 'wingtip' substituents influence the properties of such compounds in the absorption of nucleophiles such as cyanide ions. Their varied structures have led to investigations into their potential medicinal uses, thereby uncovering properties such as antimicrobial and anticancer activities (Kadafour *et al.*, 2022; Ott, 2017). Recently, we have focused on the development of imine-functionalized benzimidazolylidene compounds as potential ligands for earth-abundant metals that were utilized as homogeneous catalysts for the transfer hydrogenation of ketones (Abubakar & Bala, 2020; Kadafour & Bala, 2021). As part of our ongoing work aimed at developing new derivatives with enhanced catalytic properties, we synthesized the title compound, $C_{15}H_{14}N_3O_3^+\cdot Br^-$ (**I**), and determined its crystal structure.

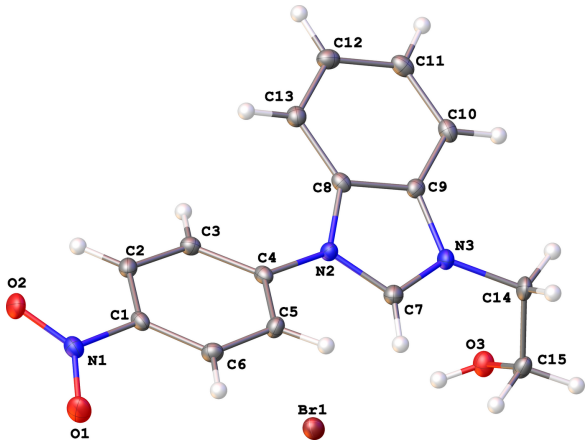

Figure 1
The molecular structure of (**I**) showing displacement ellipsoids drawn at the 50% probability level.

The asymmetric unit of (**I**) consists of a cationic benzoimidazolium species and a bromide ion as depicted in Fig. 1. In comparison with the recently reported 3-(2-hydroxyethyl)-1-(4-nitrophenyl)-1*H*-imidazol-3-ium bromide (**II**) (Ibrahim *et al.*, 2024), the presence of the benzoimidazole moiety in (**I**) seem to widen the dihedral angle between the imidazole and 4-nitrophenyl rings from 8.99 (14)° in (**II**) to 24.26 (5)° in (**I**) while causing the ethanolyl side chain to adopt a synclinal conformation with respect to the fused imidazole ring [C7—N3—C14—C15 torsion angle = 59.7 (2)°]. In the extended structure of (**I**), the bromide ion acts as a double acceptor for O3—H3*A*···Br1 and C7—H7···Br1 links (Table 1) and inversion symmetry generates tetramers (two cations and two anions) with an $R_4^2(16)$ graph-set descriptor, as shown in Fig. 2. Intermolecular C—H···O hydrogen bonds exist between atom H13 of the phenyl moiety and O3 of the hydroxy group (Fig. 2), which link the hydrogen-bonded 16-membered rings to form a two-dimensional supramolecular structure that extends diagonally with respect to the crystallographic *bc* plane (Fig. 3).

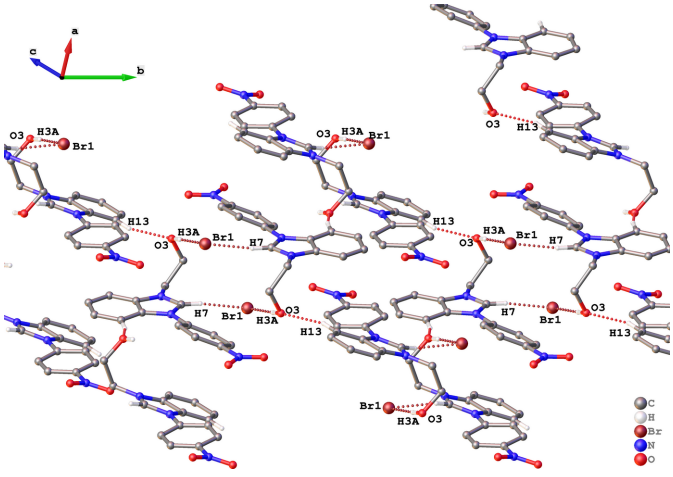

Figure 2
Representation of C7—H7···Br1, O3—H3*A*···Br1 and C13—H13···O3 hydrogen bonds (dotted bonds) in the packing of (**I**).

Table 1
Hydrogen-bond geometry (Å, °).

D—H···*A*	*D*—H	H···*A*	*D*···*A*	*D*—H···*A*
O3—H3*A*···Br1	0.84 (1)	2.39 (1)	3.2316 (11)	175
C7—H7···Br1^{i}	0.95	2.68	3.5881 (16)	161
C13—H13···O3^{ii}	0.95	2.39	3.3052 (19)	161

Symmetry codes: (i) $-x+1, -y, -z+1$; (ii) $x+\frac{1}{2}, -y+\frac{1}{2}, z+\frac{1}{2}$.

Synthesis and crystallization

The title compound was synthesized using a modified literature protocol (Ibrahim & Bala, 2016). To a Schlenk tube initially charged with *N-para* nitrophenyl benzimidazole (0.50 g, 0.0021 mol) and an excess of 2-bromoethanol (0.78 g, 0.0063 mol) was added dry acetonitrile (20 ml). The mixture was stirred and refluxed under nitrogen for 16 h. Removal of all volatiles from the greenish grey mixture and subsequent washing with batches of dry ethyl acetate (30 ml × 5) until the washing became colourless gave a grey solid, which was shown to be pure with TLC. The grey precipitate was then dried under vacuum to yield a greyish solid of the title compound. Colourless, block-shaped crystals of (**I**) suitable for crystal-structure determination were grown by the slow diffusion of diethyl ether into a methanolic solution of the title compound. Yield: 0.42 g, 55.3%. m.p. 226–228°C. ^{1}H NMR (400 MHz, DMSO-d_6): $\delta_{p.p.m.}$ 10.39 [*s*, 1H, NC(H)N], 8.67 (*d*, *J* = 8.9 Hz, 2 × 1H, CH_p), 8.31 (*d*, *J* = 7.5 Hz, 1H, CH_b), 8.21 (*d*, *J* = 8.9 Hz, 2 × 1H, CH_p), 8.02 (*d*, *J* = 8.6 Hz, 1H, CH_b), 7.87 (*m*, 2 × 1H, CH_b), 5.29 (*s*, *b*, 1H, OH_e), 4.74 (*t*, *J* = 9.8 Hz, 2H, $CH_{2\,e}$), 3.99 (*t*, *J* = 9.8 Hz, 2H, $CH_{2\,e}$): b = benzoyl, p = phenyl, e = ethanoyl. ^{13}C NMR (100 MHz, DMSO-d_6): $\delta_{p.p.m.}$ 148.1 (NCN), 143.2, 138.1, 131.5, 130.7, 127.6, 127.1, 126.6, 114.5, 113.4, 58.6 (CH_2), 50.1 (CH_2). FTIR (cm^{-1}): ν_{O-H} 3244; $\nu_{aryl\ C-H}$ 3081, $\nu_{alkyl\ C-H}$ 2997; $\nu_{C=N}$ 1566; ν_{Nitro} 1512, 1328; ν_{C-O} 1255;. LCMS (ESI$^+$): *m*/*z* (%) 284.0635 (100) [(*M*—Br)]$^+$.

Refinement

Crystallographic data and structure refinement details are summarized in Table 2.

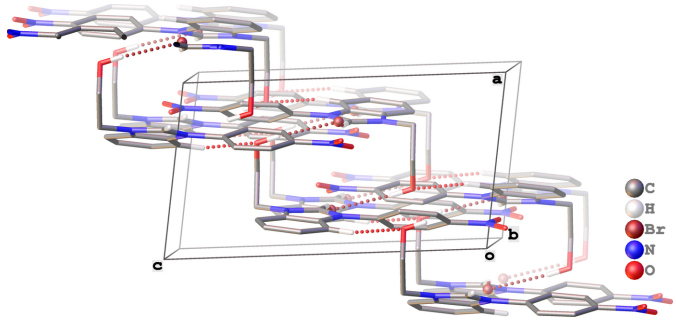

Figure 3
Representation of the propagation of the two-dimensional supramolecular structure in (**I**).

Acknowledgements

The authors would like to thank the University of KwaZulu-Natal for the research facilities. DUT/HANT is acknowledged for funding the postdoctoral fellowship of HI.

References

Abubakar, S. & Bala, M. D. (2020). *ACS Omega*, **5**, 2670–2679.
Bruker (2010). *APEX2*. Bruker AXS Inc., Madison, Wisconsin, USA.
Dolomanov, O. V., Bourhis, L. J., Gildea, R. J., Howard, J. A. K. & Puschmann, H. (2009). *J. Appl. Cryst.* **42**, 339–341.
Ibrahim, H. & Bala, M. D. (2016). *New J. Chem.* **40**, 6986–6997.
Ibrahim, H., Zamisa, S. J., Bala, M. D. & Friedrich, H. B. (2022). *Z. Kristallogr. New Cryst. Struct.* **237**, 23–25.
Ibrahim, H., Zamisa, S. J., Bala, M. D., Ntola, P. & Friedrich, H. B. (2024). *IUCrData*, **9**, x241138.
Kadafour, A. N. W. & Bala, M. D. (2021). *J. Coord. Chem.* **74**, 2886–2897.
Kadafour, A. N. W., Ibrahim, H. & Bala, M. D. (2022). *J. Mol. Struct.* **1262**, 132997–13300.
Krause, L., Herbst-Irmer, R., Sheldrick, G. M. & Stalke, D. (2015). *J. Appl. Cryst.* **48**, 3–10.
Kumar, R., Sandhu, S., Hundal, G., Singh, P., Walia, A., Vanita, V. & Kumar, S. (2015). *Org. Biomol. Chem.* **13**, 11129–11139.
Kumar, S., Singh, P., Hundal, G., Singh Hundal, M. & Kumar, S. (2013). *Chem. Commun.* **49**, 2667–2669.
Lee, H. M., Lu, C. Y., Chen, C. Y., Chen, W. L., Lin, H. C., Chiu, P. L. & Cheng, P. Y. (2004). *Tetrahedron*, **60**, 5807–5825.
Ott, I. (2017). *Medicinal Chemistry of Metal N-Heterocyclic Carbene (NHC) Complexes.* In *Inorganic and Organometallic Transition Metal Complexes with Biological Molecules and Living Cells*, edited by K. K.-W. Lo, pp. 147–179. New York: Academic Press.
Sheldrick, G. M. (2015*a*). *Acta Cryst.* A**71**, 3–8.
Sheldrick, G. M. (2015*b*). *Acta Cryst.* C**71**, 3–8.

Table 2
Experimental details.

Crystal data	
Chemical formula	$C_{15}H_{14}N_3O_3^+\cdot Br^-$
M_r	364.20
Crystal system, space group	Monoclinic, $P2_1/n$
Temperature (K)	100
a, b, c (Å)	6.7708 (1), 17.2107 (2), 12.3465 (2)
β (°)	98.184 (1)
V (Å^3)	1424.09 (4)
Z	4
Radiation type	Mo $K\alpha$
μ (mm^{-1})	2.90
Crystal size (mm)	0.32 × 0.19 × 0.13
Data collection	
Diffractometer	Bruker *SMART APEX2* CCD
Absorption correction	Multi-scan (*SADABS*; Krause et al., 2015)
T_{min}, T_{max}	0.628, 0.746
No. of measured, independent and observed [$I > 2\sigma(I)$] reflections	32857, 3555, 3006
R_{int}	0.029
$(\sin\theta/\lambda)_{max}$ (Å^{-1})	0.669
Refinement	
$R[F^2 > 2\sigma(F^2)]$, $wR(F^2)$, S	0.022, 0.057, 1.04
No. of reflections	3555
No. of parameters	202
No. of restraints	1
H-atom treatment	H atoms treated by a mixture of independent and constrained refinement
$\Delta\rho_{max}$, $\Delta\rho_{min}$ (e Å^{-3})	0.38, −0.31

Computer programs: *APEX2* (Bruker, 2010), *SHELXT2013* (Sheldrick, 2015*a*), *SHELXL2018/3* (Sheldrick, 2015*b*) and *OLEX2* (Dolomanov *et al.*, 2009).